ELSEVIER

International Conference On DESIGN AND MANUFACTURING, IConDM 2013

Dynamic Analysis and Modeling of Jansen Mechanism

Shunsuke Nansai[a,b,*], Mohan Rajesh Elara[b], Masami Iwase[a]

[a]*Department of Advanced Multidisciplinary Engineering, Tokyo Denki University, Tokyo 120-8551, Japan*
[b]*Singapore University of Technology and Design, 20 Dover Drive Singapore 138682*

Abstract

Theo Jansen mechanism is gaining wide spread popularity among legged robotics researchers due to its scalable design, energy efficiency, low payload to machine load ratio, bio-inspired locomotion, deterministic foot trajectory among others. In this paper, we present dynamic analysis of a four legged Theo Jansen link mechanism using projection method that results in constraint force and equivalent Lagrange's equation of motion necessary for any meaningful extension and/or optimization of this niche mechanism. Numerical simulations using MaTX is presented in conjunction with the dynamic analysis. This research sets a theoretical basis for future investigation into Theo Jansen mechanism.

Keywords: Jansen Mechanism, Projection Method, Dynamic Analysis

1. Introduction

Legged robots has always been a favorite for researchers where the application involves maneuverability over rough terrain, especially such priority is obvious in comparison to traditional wheeled, or tracked robotic platforms. Sebastian et al [1] present their efforts in developing a six legged, bio-inspired, and energy efficient robot, SpaceClimber 1 for extraterrestrial surface exploration, paying special attention to mobility in lunar craters. Estremera et al [2] elaborates with simulation and experiments the development of crab and turning gaits for hexpod robot, SILO-6 deployments in demining applications often characterized by uneven terrains and forbidden zones. Federico et al [3] proposes an approach to directly map a range of gaits of a horse to a quadruped robot with an intention of generating a more life-like locomotion cycle. The work also presents the use of kinematic motion primitives in generating valid and stable walking, trotting and galloping gaits that are tested on a compliant quadruped robot.

In many of these research works, the robots developed are generally highly effective in mimicking the gait cycles of their biological counterparts but they suffer from low payload to machine-load ratio and high energy consumption. Several approaches are being studied in developing energy efficient walking machines. Sanz-Meodio et al [4] presents a set of rules towards improving energy efficiency in statically stable walking robots extracted to careful dynamic simulation and analysis of two legged, mammal and insect

---

*Corresponding author. Tel.: +81-3-5284-5333.
Email address: nansai@ctrl.fr.dendai.ac.jp (Shunsuke Nansai)

configurations for a hexapod robotic platform. Gonzalez de Santos et al [5] applies minimization criteria for optimizing energy consumption in a hexapod robot over every half a locomotion cycle especially while walking on uneven terrains. Roy et al [6] put forward two different approaches to determine optimal feet forces and joint torques for six legged robots towards minimizing energy consumption. Even though these works focuses on the energy optimization problem, still the robots experimented in these works involves a series of links with multiple actuators to realize walking motion. An unconventional approach was presented by Theo Jansen [7], a Dutch kinetic artist that requires actuation at only a single joint to realize walking involving multiple legs through mapping of internal cyclic gaits into elliptical ones. Various aspects of Theo Jansen mechanism has been studied by a number of researchers. Kazuma et al [8] proposes an extension of the Theo Jansen mechanism by introducing an additional up-down motion in the linkage center for realizing new gait cycles with about ten times the height of original for climbing over obstacles. vector loop and simple geometric methods are used in conjunction with software tools such as ProEngineer and SAM for analyzing forward kinematics of the Theo Jansen mechanism by Moldovan [9]. An attempt to optimize the leg geometry of Theo Jansen mechanism using genetic algorithm is presented by Ingram et al [10]. The work explores the stability limits and tractive abilities while validating the kinematic and kinetic models through experiments involving hardware prototypes. Daniel et al [11] conducts a preliminary dynamic analysis using the superposition method with the intention of optimizing Theo Jansen mechanism. But, the work is incomplete with no details on the equivalent Lagrange's equation. A complete dynamic analysis involving constraint force and equivalent Lagrange's equation of motion are necessary for any meaningful extension and/or optimization of the Theo Jansen mechanism.

In this paper, we present a complete dynamic analysis of the Theo Jansen mechanism using the projection method proposed by Blajer [12]. In comparison to the conventional approaches of Lagrange's, Gibbs-Appel, and Kane's, the projection method utilized in this paper has been observed to be intuitive in nature and compact (Arczewski et al. [13], Maruyama [14], Ohsaki et al. [15]). The work presented in this paper is part of our ongoing efforts in developing a nested reconfigurable Theo Jansen mechanism which is capable of both inter- and intra- reconfiguration capabilities. With Theo Jansen mechanism at its core, the platform being developed is expected to possess individual robots capable of changing their morphologies (intra-reconfigurability) as well as combining with other homogeneous/heterogeneous robots to generate more complex morphologies (inter-reconfigurability). In Summary, we hypothesize that the research and development of nested reconfigurable Theo Jansen mechanism robot has high academic value and practical impact. For which, complete dynamics analysis of Theo Jansen mechanism is an essential but complex step. Therefore, the dynamic analysis is conducted in this paper using the projection method.

The paper is organized as follows. In Section 2, the dynamic modeling of Jansen linkage is presented that consists of Forepaw and backpaw modeling cum complete system equations. In Section 3, numerical simulation preformed using MaTX are presented. Finally, concluding remarks are presented in Section 4.

2. Modeling of Jansen Linkage

A schematic figure of the jansen link mechanism is shown in Fig. 1. As shown in Fig. 1, the jansen link mechanism under study in this paper is a four legged model that can be actuated with only one motor, where input torque is driven to driving link. And, the driving link is constrained on origin of the Descartes coordinates. Also, the same jansen link mechanisms is utilized for constructing the other legs of the robot. Hence, the motion equations of the Theo Jansen mechanism modelled as a system can be derived by integrating the component motion equations of forepaw and backpaw models. In this paper, the motion equations of forepaw are derived as a first step, and then the ones of backpaw are derived in the second step. Finally, the motion equations of the whole system are derived integrating the motion equations of the prior.

2.1. Forepaw Modeling

A dynamic model of a forepaw of a Jansen linkage mechanism is derived in this Section. The schematic figure and coordinate systems of the robot are illustrated in Fig. 2, and its parameters are tabulated in Table 1. Fig. 2 shows single Jansen linkage mechanism with unfixed driving link. The length of each link adopted
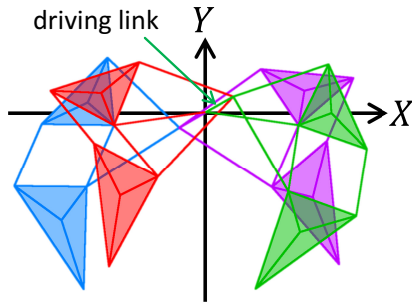
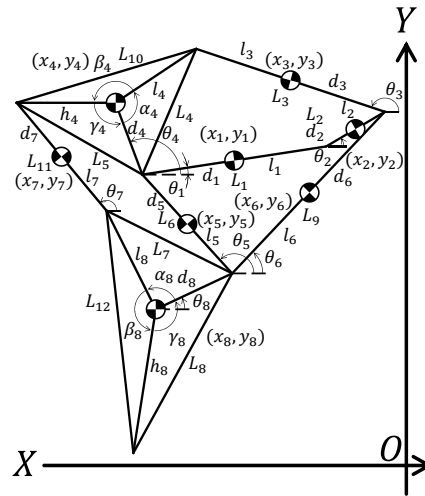Fig. 1. Schematic figure of a four legged jansen linkage mechanism

Fig. 2. Schematic figure of forepow of a jansen linkage mechanism

Table 1. Physical parameters ($i = 1, \cdots, 8, j = 1, \cdots, 8, k = 1, \cdots, 12$).

Parameters	Notation	Value
Inertia moment [kg·m^2]	J_i	0.1
Mass [m]	m_i	0.1
Viscous friction coefficient [Nm·s/rad]	C_{ij}	0.1
Length of (x, y)-coordinate of link-1 [m]	(l_0, h_0)	(0.32436, 0.04632)
Length of link	L_k	
Length from extermity to center of gravity [m]	d_i	
Length from center of gravity to end [m]	l_i	
Length from center of gravity to corner of triangle [m]	$d_{4,8}, l_{4,8}, h_{4,8}$	
Angle between center of gravity to corner of triangle [m]	$\alpha_{4,8}, \beta_{4,8}, \gamma_{4,8}$	

for the design under study in relation to Fig. 2 are listed as $L_1 = 0.32436$ m, $L_2 = 0.10834$ m, $L_3 = 0.34885$ m, $L_4 = 0.23529$ m, $L_5 = 0.25134$ m, $L_6 = 0.23508$ m, $L_7 = 0.25342$ m, $L_8 = 0.35948$ m, $L_9 = 0.38322$ m, $L_{10} = 0.32338$ m, $L_{11} = 0.23934$ m and $L_{12} = 0.43599$ m (Nansai et al. [16]). It is assumed that the center of gravity of every link exists on the center of the specified link. Also, the center of gravity of the triangle present in the design exist on vertex of three median line. The angle between center of gravity to corner of triangle and the length from center of gravity to corner of triangle are calculated as $d_4 = 0.122562$ m, $l_4 = 0.170599$ m, $h_4 = 0.178215$ m, $d_8 = 0.147877$ m, $l_8 = 0.205316$ m, $h_8 = 0.252632$ m, $\alpha_4 = 1.87097$ rad, $\beta_4 = 2.4248$ rad, $\gamma_4 = 1.98742$ rad, $\alpha_8 = 1.57408$ rad, $\beta_8 = 2.51629$ rad and $\gamma_8 = 2.19281$ rad respectively utilizing the law of cosines.

First of all, a constraint-free model is derived from Fig. 2 with parameters in Table 1. The generalized coordinate of this system is defined as

$$\mathbf{x_{pf}} = \begin{bmatrix} \theta_1 & x_1 & y_1 & \theta_2 & x_2 & y_2 & \cdots & \theta_8 & x_8 & y_8 \end{bmatrix}^T, \tag{1}$$

where subscript f represents forepaw. The translational motion and rotational motion of each constraint-free object that forms the robot can be easily derived as equations of motion. The equations of motion concerned with each objects are represented in the vector form (2) with the generalized coordinate (1) as presented below,

$$\mathbf{M_f \ddot{x}_{pf} = h_f}, \tag{2}$$

where a generalized mass matrix $\mathbf{M_f}$ and a generalized force matrix $\mathbf{h_f}$ are defined as

$$\mathbf{M_f} = \mathrm{diag}(J_1, m_1, m_1, J_2, m_2, m_2, \cdots, J_8, m_8, m_8),$$

$$\mathbf{h_f} = \begin{bmatrix}
-\tau + C_{12}(\dot{\theta}_2 - \dot{\theta}_1) \\
0 \\
-m_1 g \\
\tau - C_{12}(\dot{\theta}_2 - \dot{\theta}_1) + C_{23}(\dot{\theta}_3 - \dot{\theta}_2) \\
0 \\
-m_2 g \\
-C_{23}(\dot{\theta}_3 - \dot{\theta}_2) + C_{34}(\dot{\theta}_4 - \dot{\theta}_3) + C_{36}(\dot{\theta}_6 - \dot{\theta}_3) \\
0 \\
-m_3 g \\
-C_{14}(\dot{\theta}_4 - \dot{\theta}_1) - C_{34}(\dot{\theta}_4 - \dot{\theta}_3) + C_{45}(\dot{\theta}_5 - \dot{\theta}_4) + C_{47}(\dot{\theta}_7 - \dot{\theta}_4) \\
0 \\
-m_4 g \\
-C_{45}(\dot{\theta}_5 - \dot{\theta}_4) + C_{56}(\dot{\theta}_6 - \dot{\theta}_5) + C_{58}(\dot{\theta}_8 - \dot{\theta}_5) \\
0 \\
-m_5 g \\
-C_{36}(\dot{\theta}_6 - \dot{\theta}_3) - C_{56}(\dot{\theta}_6 - \dot{\theta}_5) + C_{68}(\dot{\theta}_8 - \dot{\theta}_6) \\
0 \\
-m_6 g \\
-C_{47}(\dot{\theta}_7 - \dot{\theta}_4) + C_{78}(\dot{\theta}_8 - \dot{\theta}_7) \\
0 \\
-m_7 g \\
-C_{68}(\dot{\theta}_8 - \dot{\theta}_6) - C_{78}(\dot{\theta}_8 - \dot{\theta}_7) \\
0 \\
-m_8 g
\end{bmatrix},$$

where τ represents the input torque from actuator.

In the next step, the constraint matrix $\mathbf{C_f}$ which holds $\mathbf{C_f \dot{x}_{pf}} = \mathbf{0}$ is derived from constraint conditions. About the position of the center of gravity of each link, the holonomic constraints are represented as follows,

$$\mathbf{\Phi_{hf}} = \begin{bmatrix}
x_2 - x_1 - d_1 \cos\theta_1 - d_2 \cos\theta_2 \\
y_2 - y_1 - d_1 \sin\theta_1 - d_2 \sin\theta_2 \\
x_3 - x_2 - d_2 \cos\theta_2 - d_3 \cos\theta_3 \\
y_3 - y_2 - d_2 \sin\theta_2 - d_3 \sin\theta_3 \\
x_4 - x_3 - d_3 \cos\theta_3 - l_4 \cos(\theta_4 + \alpha_4) \\
y_4 - y_3 - d_3 \sin\theta_3 - l_4 \sin(\theta_4 + \alpha_4) \\
x_4 - x_1 + d_1 \cos\theta_1 - d_4 \cos\theta_4 \\
y_4 - y_1 + d_1 \sin\theta_1 - d_4 \sin\theta_4 \\
x_5 - x_1 + d_1 \cos\theta_1 + d_5 \cos\theta_5 \\
y_5 - y_1 + d_1 \sin\theta_1 + d_5 \sin\theta_5 \\
x_6 - x_5 + l_5 \cos\theta_5 - l_6 \cos\theta_6 \\
y_6 - y_5 + l_5 \sin\theta_5 - l_6 \sin\theta_6 \\
x_6 - x_2 - l_2 \cos\theta_2 + d_6 \cos\theta_6 \\
y_6 - y_2 - l_2 \sin\theta_2 + d_6 \sin\theta_6 \\
x_7 - x_4 + h_4 \cos(\theta_4 - \gamma_4) - d_7 \cos\theta_7 \\
y_7 - y_4 + h_4 \sin(\theta_4 - \gamma_4) - d_7 \sin\theta_7 \\
x_8 - x_5 + l_5 \cos\theta_5 + d_8 \cos\theta_8 \\
y_8 - y_5 + l_5 \sin\theta_5 + d_8 \sin\theta_8 \\
x_8 - x_7 - l_7 \cos\theta_7 + l_8 \cos(\theta_8 + \alpha_8) \\
y_8 - y_7 - l_7 \sin\theta_7 + l_8 \sin(\theta_8 + \alpha_8)
\end{bmatrix} = \mathbf{0}.$$

The constraint matrix is defined as

$$\mathbf{C_f} := \frac{\partial \mathbf{\Phi_{hf}}}{\partial \dot{\mathbf{x}}_{pf}}.$$

(3)

The constraint dynamical system can thus be represented by adding the constraint term with Lagrange's multipliers λ to (2) as

$$\mathbf{M_f}\ddot{\mathbf{x}}_{pf} = \mathbf{h_f} + \mathbf{C_f}^\mathbf{T}\lambda_\mathbf{f},$$

(4)

utilizing (3). The degree of freedom of the unconstraint system is found to be 24 from (1). The degree of freedom should be constrained by 20 holonomic constraints in this system. Therefore, the degree of freedom of the constrained dynamical system is 4. The tangent speed of the constrained system is denoted as,

$$\dot{\mathbf{q}}_\mathbf{f} = \begin{bmatrix} \dot{\theta}_1 & \dot{x}_1 & \dot{y}_1 & \dot{\theta}_2 \end{bmatrix}^T.$$

Setting a partition symbolically as $\mathbf{v} = \begin{bmatrix} \dot{\mathbf{q}}_\mathbf{f}^T & \mathbf{v_{fD}}^\mathbf{T} \end{bmatrix}^\mathbf{T}$ where $\mathbf{v_{fD}}$ shows dependent velocities with respect to $\dot{\mathbf{q}}_\mathbf{f}$. $\mathbf{C_f}$ is decomposed into $\mathbf{C_f} = \begin{bmatrix} \mathbf{C_{f1}} & \mathbf{C_{f2}} \end{bmatrix}$ satisfying $\mathbf{C_f}\dot{\mathbf{x}}_{pf} = \mathbf{C_{f1}}\dot{\mathbf{q}}_\mathbf{f} + \mathbf{C_{f2}}\mathbf{v_{fD}}$. $\mathbf{D_f}$ is the orthogonal complement matrix to $\mathbf{C_f}$ satisfying $\mathbf{C_f}\mathbf{D_f} = \mathbf{0}$ and $\dot{\mathbf{x}}_{pf} = \mathbf{D_f}\dot{\mathbf{q}}_\mathbf{f}$ is represented by $\mathbf{D_f}$,

$$\mathbf{D_f} = \begin{bmatrix} \mathbf{I^{4 \times 4}} \\ -\mathbf{C_{f2}}^{-1}\mathbf{C_{f1}} \end{bmatrix},$$

where $\mathbf{I^{4 \times 4}}$ represents the identity matrix of 4×4.

Finally, multiplying (4) by $\mathbf{D_f}^\mathbf{T}$ from the left-hand side and substituting the coordinate transformation $\dot{\mathbf{x}}_{pf} = \mathbf{D_f}\dot{\mathbf{q}}_\mathbf{f}$ into (4), the constraint term with $\lambda_\mathbf{f}$ can be vanished, and the reduced robot equations of motion in Fig. 2 is derived as

$$\mathbf{D_f}^\mathbf{T}\mathbf{M_f}\mathbf{D_f}\ddot{\mathbf{q}}_\mathbf{f} + \mathbf{D_f}^\mathbf{T}\mathbf{M_f}\dot{\mathbf{D}}_\mathbf{f}\dot{\mathbf{q}}_\mathbf{f} = \mathbf{D_f}^\mathbf{T}\mathbf{h_f}.$$

(5)

2.2. Backpaw Modeling

Motion equations of backpaw are derived in this Section. The schematic model of backpaw is shown in Fig. 3. The physical parameters utilized for the backpaw are identical to the ones in Table 1. The motion equations of backpaw are again identical to the ones of the forepaw except for the constraint conditions that
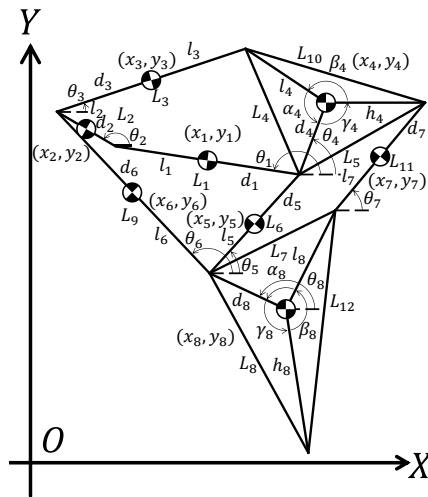

Fig. 3. Schematic figure of backpow of a jansen linkage mechanism

exists in both cases are different. The subscript b is utilized to discriminate parameters for forepaw and backpaw. The holonomic constraints are represented as follows,

$$\boldsymbol{\Phi_{hb}} = \begin{bmatrix} x_2 - x_1 - d_1 \cos\theta_1 - d_2 \cos\theta_2 \\ y_2 - y_1 - d_1 \sin\theta_1 - d_2 \sin\theta_2 \\ x_3 - x_2 - d_2 \cos\theta_2 - d_3 \cos\theta_3 \\ y_3 - y_2 - d_2 \sin\theta_2 - d_3 \sin\theta_3 \\ x_4 - x_3 - d_3 \cos\theta_3 - l_4 \cos(\theta_4 - \alpha_4) \\ y_4 - y_3 - d_3 \sin\theta_3 - l_4 \sin(\theta_4 - \alpha_4) \\ x_4 - x_1 + d_1 \cos\theta_1 - d_4 \cos\theta_4 \\ y_4 - y_1 + d_1 \sin\theta_1 - d_4 \sin\theta_4 \\ x_5 - x_1 + d_1 \cos\theta_1 + d_5 \cos\theta_5 \\ y_5 - y_1 + d_1 \sin\theta_1 + d_5 \sin\theta_5 \\ x_6 - x_5 + l_5 \cos\theta_5 - l_6 \cos\theta_6 \\ y_6 - y_5 + l_5 \sin\theta_5 - l_6 \sin\theta_6 \\ x_6 - x_2 - l_2 \cos\theta_2 + d_6 \cos\theta_6 \\ y_6 - y_2 - l_2 \sin\theta_2 + d_6 \sin\theta_6 \\ x_7 - x_4 + h_4 \cos(\theta_4 + \gamma_4) - d_7 \cos\theta_7 \\ y_7 - y_4 + h_4 \sin(\theta_4 + \gamma_4) - d_7 \sin\theta_7 \\ x_8 - x_5 + l_5 \cos\theta_5 + d_8 \cos\theta_8 \\ y_8 - y_5 + l_5 \sin\theta_5 + d_8 \sin\theta_8 \\ x_8 - x_7 - l_7 \cos\theta_7 + l_8 \cos(\theta_8 - \alpha_8) \\ y_8 - y_7 - l_7 \sin\theta_7 + l_8 \sin(\theta_8 - \alpha_8) \end{bmatrix} = \boldsymbol{0}.$$

As dealth with earlier in the case of forepaw modelling, the constraint matrix is firstly decomposed, then the orthogonal complement matrix is derived and finally the motion equations of the backpaw are derived as follows,

$$\mathbf{D_b^T M_b D_b \ddot{q}_b + D_b^T M_b \dot{D}_b \dot{q}_b = D_b^T h_b}. \tag{6}$$

2.3. System Integration

Motion equations of the complete four legged jansen link mechanism is derived utilizing (5) and (6). Two motion equations are utilized namely (5) and (6) that represents the motion equations of only one leg. A fixed model is utilized to analyse dynamical behavior of this link mechanism. The motion equations of right and left forepaw are represented as follows,

$$\mathbf{D_{rf}^T M_{rf} D_{rf} \ddot{q}_{rf} + D_{rf}^T M_{rf} \dot{D}_{rf} \dot{q}_{rf} = D_{rf}^T h_{rf}}, \tag{7}$$

$$\mathbf{D_{lf}^T M_{lf} D_{lf} \ddot{q}_{lf} + D_{lf}^T M_{lf} \dot{D}_{lf} \dot{q}_{lf} = D_{lf}^T h_{lf}}, \tag{8}$$

by (5). Where subscript r and l represents right-leg and left-leg respectively Also, The ones of right and left backpaw are represented as follows

$$\mathbf{D_{rb}^T M_{rb} D_{rb} \ddot{q}_{rb} + D_{rb}^T M_{rb} \dot{D}_{rb} \dot{q}_{rb} = D_{rb}^T h_{rb}}, \tag{9}$$

$$\mathbf{D_{lb}^T M_{lb} D_{lb} \ddot{q}_{lb} + D_{lb}^T M_{lb} \dot{D}_{lb} \dot{q}_{lb} = D_{lb}^T h_{lb}}, \tag{10}$$

by (6).

When the four legs aren't constrained, the motion equations of the system are represents as follows,

$$\mathbf{M}\ddot{\mathbf{x}}_{\mathbf{p}} = \mathbf{h} \tag{11}$$

$$\mathbf{x}_{\mathbf{p}} = \begin{bmatrix} \mathbf{q}_{\mathbf{rf}}^{\mathbf{T}} & \mathbf{q}_{\mathbf{lf}}^{\mathbf{T}} & \mathbf{q}_{\mathbf{rb}}^{\mathbf{T}} & \mathbf{q}_{\mathbf{lb}}^{\mathbf{T}} \end{bmatrix}^{T},$$

$$\mathbf{M} = \mathrm{diag}(\mathbf{D_{rf}}^{\mathbf{T}}\mathbf{M_{rf}}\mathbf{D_{rf}}, \mathbf{D_{lf}}^{\mathbf{T}}\mathbf{M_{lf}}\mathbf{D_{lf}}, \mathbf{D_{rb}}^{\mathbf{T}}\mathbf{M_{rb}}\mathbf{D_{rb}}, \mathbf{D_{lb}}^{\mathbf{T}}\mathbf{M_{lb}}\mathbf{D_{lb}}),$$

$$\mathbf{h} = \begin{bmatrix} (\mathbf{D_{rf}}^{\mathbf{T}}\mathbf{h_{rf}} - \mathbf{D_{rf}}^{\mathbf{T}}\mathbf{M_{rf}}\dot{\mathbf{D}}_{\mathbf{rf}}\dot{\mathbf{q}}_{\mathbf{rf}})^{\mathbf{T}} \\ (\mathbf{D_{lf}}^{\mathbf{T}}\mathbf{h_{lf}} - \mathbf{D_{lf}}^{\mathbf{T}}\mathbf{M_{lf}}\dot{\mathbf{D}}_{\mathbf{lf}}\dot{\mathbf{q}}_{\mathbf{lf}})^{\mathbf{T}} \\ (\mathbf{D_{rb}}^{\mathbf{T}}\mathbf{h_{rb}} - \mathbf{D_{rb}}^{\mathbf{T}}\mathbf{M_{rb}}\dot{\mathbf{D}}_{\mathbf{rb}}\dot{\mathbf{q}}_{\mathbf{rb}})^{\mathbf{T}} \\ (\mathbf{D_{lb}}^{\mathbf{T}}\mathbf{h_{lb}} - \mathbf{D_{lb}}^{\mathbf{T}}\mathbf{M_{lb}}\dot{\mathbf{D}}_{\mathbf{lb}}\dot{\mathbf{q}}_{\mathbf{lb}})^{\mathbf{T}} \end{bmatrix},$$

by (7), (8), (9) and (10).

About the center of gravity of each link, the holonomic constraints are represented as follows,

$$\mathbf{\Phi_h} = \begin{bmatrix} x_{rf1} + l_{rf1}\cos\theta_{rf1} \\ y_{rf1} + l_{rf1}\sin\theta_{rf1} \\ \theta_{rf1} - \tan^{-1}(l_0/h_0) \\ \theta_{rb1} - \theta_{rf1} + 2\tan^{-1}(l_0/h_0) - \pi \\ x_{rb1} - x_{rf1} - l_{rf1}\cos\theta_{rf1} + d_{rb1}\cos\theta_{rb1} \\ y_{rb1} - y_{rf1} - l_{rf1}\sin\theta_{rf1} + d_{rb1}\sin\theta_{rb1} \\ \theta_{rb2} - \theta_{rf2} \\ \theta_{lf1} - \theta_{rf1} \\ x_{lb1} - x_{lf1} \\ y_{lb1} - y_{lf1} \\ \theta_{lf2} - \theta_{rf2} + \pi \\ \theta_{lb1} - \theta_{lf1} + 2\tan^{-1}(l_0/h_0) - \pi \\ x_{lb1} - x_{lf1} - l_{lf1}\cos\theta_{lf1} + d_{lb1}\cos\theta_{lb1} \\ y_{lb1} - y_{lf1} - l_{lf1}\sin\theta_{lf1} + d_{lb1}\sin\theta_{lb1} \\ \theta_{lb2} - \theta_{lf2} \end{bmatrix} = \mathbf{0}.$$

The degree of freedom of the unconstraint system is 16 from (11). The degree of freedom should be constrained by 15 holonomic constraints in this system. Therefore, the degree of freedom of the constraint dynamical system is 1. The tangent speed of the constraint system is denoted as,

$$\dot{\mathbf{q}} = \begin{bmatrix} \dot{\theta}_{rf2} \end{bmatrix}.$$

As computed previously for the case of the modeling of forepaw, the constraint matrix is decomposed first, followed by the derivation of orthogonal complement matrix and then derivation of the motion equations of the four legged jansen link mechanism as follows,

$$\mathbf{D^T M D \ddot{q}} + \mathbf{D^T M \dot{D} \dot{q}} = \mathbf{D^T h}. \tag{12}$$

3. Numerical Simulation

This section analyzes the dynamical behavior of the Theo Jansen leg mechanism through numerical simulation utilizing the derived motion equations. A PID controller (13) is utilized as a control system for that purpose,

$$\tau = k_p e + k_i \int e + k_d \dot{e}, \tag{13}$$

$$e = r - \theta_{rf1}, \qquad r = t + \pi, \qquad k_p = 10, \qquad k_i = 1, \qquad k_d = 1,$$

because PID controller can be controlled without any dynamics, that is, the dynamics of the Jansen link mechanism are attended pronouncedly in the numerical simulation result. The simulations are performed using MaTX with Visual C++ 2005 version 5.3.37 (Koga [17]). For the analysis presented in this paper, the simulation time was 10 seconds, and the sampling interval was 0.01 second. The initial state of the jansen link mechanism was assumed to be at $\theta_{rf1} = \pi$ rad. And, Each link and triangle are called link $i, (i = 1, \cdots, 8)$ according to subscript of generalized coordinate

4. Simulation Result and Consideration

The results from the numerical simulations are presented in Figs. 4-9.

From Fig. 4, it can be clearly confirmed that the peak of the input torque appear periodically on steady state. However, the input torque is almost constant at around -0.9 Nm except the case when the rotation speed is a constant. From the analysis, it can be concluded that in general a constant speed rotation can be maintained with a constant input torque without any complicated considerations for the system dynamics.

From Fig. 5 which shows the symmetric trajectories of the toes of the Jansen linkage mechanism, it can be concluded that a stable walking behaviour could be realized with ease given the similarity of the prior to the human walking gaits. However, Fig. 6 shows that the time variation of x-coordinate between
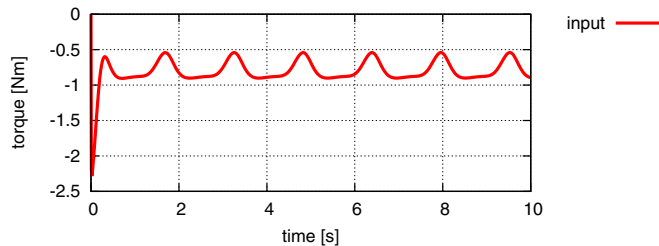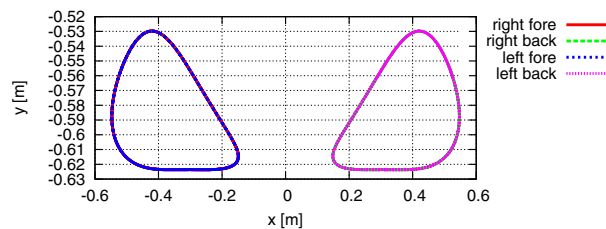

Fig. 4. The time variation of the input torque

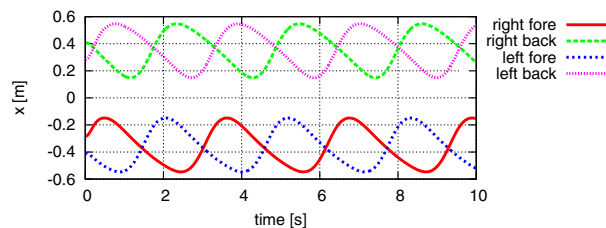Fig. 5. Trajectories of the toes of the jansen linkage mechanism

Fig. 6. The time variation of *x*-coordinate of the toes of the jansen linkage mechanism
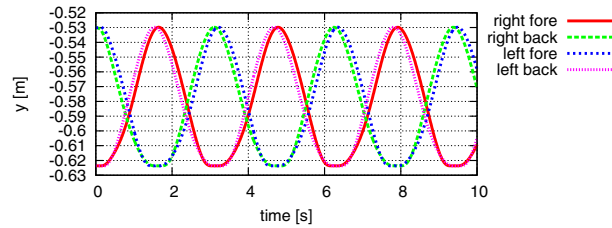
Fig. 7. The time variation of *y*-coordinate of the toes of the jansen linkage mechanism
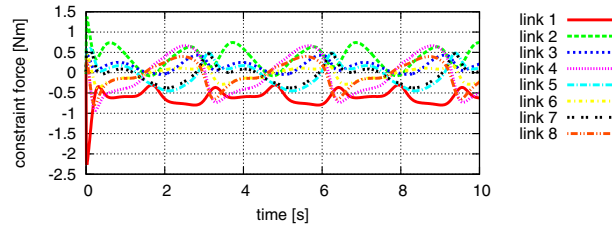

Fig. 8. The time variation of constraint forces to the rotational direction on the right-forepow
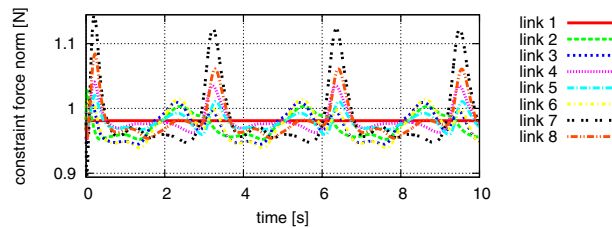

Fig. 9. The time variation of constraint forces norm to the translational direction on the right-forepow

forepaw and backpaw are not identical and there exists some differences. It represents that each toe moves with different speed consistently. As a result, it is expected for at least one leg to slip absolutely although both the legs tread the ground equally. It is commonly preferred to restrict toe slipping in walking robots regardless of biped or multi-legged platforms. However, the analysis results from Fig. 6 shows that a robot utilizing jansen link mechanism can't walk without toe slipping. Therefore, toe slipping have to be allowed while the walking control system is designed for the platform.

From Fig. 7 which presents the time variation of y-coordinate of the toes of the Jansen linkage mechanism, it is obvious to find a 0.03 m difference between the lowest point of each leg. This observation concludes that an 0.03 m up- and down- motion is expected in a robot realized using a four legged jansen link mechanism. However, this up-and-down motion can be vanished by increasing the number of legs and decreasing the phase difference.

Fig. 8 and Fig. 9 represents the constraint forces of the system, that is, forces in the constrained directions. These figures represents the forces which occur to connect the links as the constraints of this system are only the holonomic in nature. It also represents load forces to the links that are essential parameters needed in desingning an efficient robot hardware. In fact, if the observed constraint forces are large, then the robots have to be designed to be robust and solid to prevent any breakdown during operation. From Fig. 8 and Fig. 9, it is clear that the constraint force to the rotational direction for the 1st-link is the largest and the one to the translation direction for 7th-link is the largest. Therefore, steps needs to be taken to

ensure sufficient strength in 1st and 7th link to withstand the larger forces expected on them while real time deployments.

In Summary, the result of the numerical simulation concludes that the jansen link mechanism can be moved on roughly constant speed with constant input torque. It has been determined to accomodate for toe slipping while desinging the walking control system for the robot platform. Analysis has also shown that a choice of more than four legs is a must to vanish an expected up- and down- motion. Finally, care must be taken in robot developmental stage to ensure sufficient strength for the 1st and 7th link given the larger force expected on the same in order to avoid any breakdown of linkage during operation.

5. Conclusion

The paper analyzes the dynamics of a four legged Theo Jansen mechanism robot using projection method. The motion equation of the four legged platform has been derived thorugh individual modelling of forepaw and backpaw and eventual integration of the two towards a complete system model. The unified dynamics experssions together with the numerical simulation, its analysis and results provides a solid foundation for the dynamics of the Theo Jansen mechanism. This research sets a theoritical basis for further investigation, optimization or extension of the Theo Jansen mechanism, our ongoing efforts in developing a reconfigurable Theo Jansen mechanism and any potential application of the same for real world scenarios.

Acknowledgements

References

[1] Bartsch, Sebastian, Timo Birnschein, Malte Römmermann, Jens Hilljegerdes, Daniel Kühn, and Frank Kirchner. "Development of the six-legged walking and climbing robot SpaceClimber." Journal of Field Robotics 29, no. 3 (2012): 506-532.

[2] Estremera, J., J. A. Cobano, and Pablo Gonzalez de Santos. "Continuous free-crab gaits for hexapod robots on a natural terrain with forbidden zones: An application to humanitarian demining." Robotics and Autonomous Systems 58, no. 5 (2010): 700-711.

[3] Moro, Federico L., Alexander Spröwitz, Alexandre Tuleu, Massimo Vespignani, Nikos G. Tsagarakis, Auke J. Ijspeert, and Darwin G. Caldwell. "Horse-like walking, trotting, and galloping derived from kinematic Motion Primitives (kMPs) and their application to walk/trot transitions in a compliant quadruped robot."Biological Cybernetics (2013): 1-12.

[4] Sanz-Merodio, D., E. Garcia, and P. Gonzalez-de-Santos. "Analyzing energy-efficient configurations in hexapod robots for demining applications." Industrial Robot: An International Journal 39, no. 4 (2012): 357-364.

[5] de Santos, P. Gonzalez, E. Garcia, R. Ponticelli, and M. Armada. "Minimizing energy consumption in hexapod robots." Advanced Robotics 23, no. 6 (2009): 681-704.

[6] Roy, Shibendu Shekhar, and Dilip Kumar Pratihar. "Dynamic modeling, stability and energy consumption analysis of a realistic six-legged walking robot."Robotics and Computer-Integrated Manufacturing (2012).

[7] Jansen, Theo. The great pretender. Nai010 Publishers, 2007.

[8] Komoda, Kazuma, and Hiroaki Wagatsuma. "A proposal of the extended mechanism for Theo Jansen linkage to modify the walking elliptic orbit and a study of cyclic base function."

[9] Moldovan, Florina, and Valer Dolga. "Analysis of Jansen walking mechanism using CAD." Solid State Phenomena 166 (2010): 297-302.

[10] Ingram, Anthony James. "A new type of walking machine." PhD diss., 2008.

[11] Giesbrecht, Daniel, and C. Qiong Wu. "Dynamics of Legged Walking Mechanism "Wind Beast"." Department of Mechanical and Manufacturing Engineering, University of Manitoba, California (2010).

[12] Blajer, Wojciech. "A projection method approach to constrained dynamic analysis." Journal of applied Mechanics 59, no. 3 (1992): 643-649.

[13] K. Arczewski and W. Blajer, A Unified Approach to the Modelling of Holonomic and Nonholonomic Mechanical Systems, Mathematical and Computer Modelling of Dynamical Systems. Vol. 2, Issue 3, pp. 157-174, 1996.

[14] T. Maruyama, A Modeling of a Snake-like Robot, Master thesis, Graduate School of Science and Engineering, Tokyo Denki University. Vol. 24, pp. 181-184, 2005.

[15] H. Ohsaki, M. Iwase, T. Sadahiro and S. Hatakeyama, A Consideration fo Human-Unicycle Model for Unicycle Operation Analysis based on Moment Balancing Point, Proc. of SMC. San Antonio, TX, USA, October, 2009.

[16] S. Nansai, N. Rojas, M. R. Elara and R. Sosa, Exploration of Adaptive Gait Patterns with a Reconfigurable Linkage Mechanism, Proc. of IROS 2013, IEEE, submitted.

[17] M. Koga, MaTX/RtMaTX: A Freeware for Integrated CACSD, Proc. of CACSD 1999, pp. 451-456, 1999.